
Monte Carlo Simulations of Model Nonionic Surfactants

A.P. Chatterjee and A.Z. Panagiotopoulos

Institute for Physical Science & Technology,
University of Maryland,
College Park, Maryland 20742, USA

Abstract. The focus of this work is on aggregation and micellization in a lattice model for nonionic surfactants. Formation of micellar aggregates as a function of temperature and surfactant chemical potential was studied by histogram reweighting grand canonical Monte Carlo simulations. Two different sets of site-site interactions were utilized. The critical micellar concentration (CMC) was determined from the equation of state obtained from simulations in small systems. Results were obtained for the micellar size distributions. The introduction of effective repulsive site-site interactions between nearest-neighbour head-head and head-tail groups, in addition to the attractive tail-tail segmental interactions considered in earlier investigations, was shown to cause a significant decrease in the CMC. It was also found to attenuate the dependence of micellar size on surfactant chemical potential. The observed dependence of the CMC on temperature for the present model disagrees with experimental results for the *n*-alkyl *m*-ethoxyl series of surfactants in water. This is attributable to the failure of the model to take into account the (entropic) hydrophobic effect important for amphiphilic aggregation in aqueous solutions.

1 Introduction

The formation of self-assembled aggregates in aqueous solutions of amphiphiles has been investigated using experimental and theoretical methods [1–4], and, more recently, computer simulation studies [5–9]. As the surfactant concentration is increased at a fixed temperature, various macroscopic properties of the solution, e.g. the electrical conductivity or osmotic pressure, show abrupt changes in their dependence on surfactant concentration [3]. These changes are associated with the formation of mesoscopically ordered amphiphilic aggregates, which may be of spherical, cylindrical, or lamellar architecture. The overall surfactant concentration at which such aggregates first form is defined as the critical micellar concentration (CMC). The CMC generally depends on temperature, surfactant architecture and the presence of additional components in solution. For overall surfactant concentrations above the CMC, the concentration of free (monomeric) amphiphiles in the bulk is observed to be relatively constant, and the added surfactant leads to an increase in the number or size of the micellar aggregates. Formation of mesoscopically ordered microphases has been studied extensively for the case of relatively high molecular weight diblock copolymer systems [10]. Such

systems may be regarded as amphiphiles with a large degree of polymerization and exhibit very rich phase behavior at temperatures low enough that the incompatibility between the segments in the individual blocks leads to microphase separation [12].

In recent years, several computer simulation based studies have examined the aggregation process for amphiphiles of lower molecular weight (compared to block copolymeric systems) for surfactant molecules having both linear as well as “gemini” architectures. The pioneering studies in this context were initiated by R.G. Larson [13], who examined equilibria between surfactant microphases at relatively low temperatures and high surfactant volume fractions using lattice Monte Carlo simulations performed in the canonical (constant NVT) ensemble for model molecules with short-ranged nearest-neighbor interactions. More recently, the greater flexibility of the grand canonical ensemble (constant μVT conditions) together with histogram reweighting techniques have been employed in the low (near CMC) surfactant concentration regime to investigate the onset of micellization and the dependence of the CMC on temperature [9]. These studies have focussed primarily on model amphiphilic molecules of symmetric architecture, and a single fixed choice of the microscopic interactions describing head-head, head-tail, and tail-tail interactions has been employed. The present study explores a situation in which the model surfactant molecule may be of asymmetric structure, reflecting the relative volumes of head and tail group segments of real experimental hydrophobic and hydrophilic moieties, and also investigates in a preliminary manner the effects of using a different choice of microscopic interaction strengths.

2 Models and Methods

The model studied consists of linear amphiphile molecules, each occupying a set of connected sites on a simple cubic lattice. All vacant sites, i.e., those that are not occupied by either hydrophilic head (H) or hydrophobic tail (T) sites, are considered to be occupied by structureless solvent particles. The specific amphiphilic molecule we investigate in this study has the structure H_9T_6 ; if we identify each lattice site as having a volume of approximately $\approx 60\text{\AA}^3$, this structure has head and tail group volumes which correspond roughly to those of the hydrophilic and hydrophobic portions of the nonionic n -dodecyl octaoxyethylene glycol ether surfactant $C_{12}E_8$, the aggregation of which has been extensively investigated experimentally under aqueous conditions [14].

Two sets of site-site interaction sets were studied; in both cases, the only interactions assumed to be present (besides excluded volume) were between nearest-neighbor head-head (HH), head-tail (HT), and tail-tail (TT) contacts, where the set of nearest-neighbours of a given site refers to the 26 locations given by the relative vectors $(1,0,0)$, $(1,1,0)$, $(1,1,1)$, and their symmetry-equivalent analogues. Periodic boundary conditions are employed in all direc-

tions. The first interaction set employed in this work (denoted I1) corresponds to the choice used in earlier work on related models for other, shorter, amphiphile chains, and specifies the pairwise additive thermal interactions as being $[0,0,-1.3333]$ for the HH, HT, and TT interactions, respectively. Interaction set I1 thus includes only attractive tail-tail interactions; the only head-head and head-tail interactions present are purely of the excluded volume type, as only a single mer is permitted to occupy a given lattice site. The specific value for the TT attractive interaction used in this work was chosen to maintain equality of the thermal chi-parameter on a per-amphiphile basis with earlier work on surfactants with the H_4T_4 architecture, which had employed the interaction set $[0,0,-2]$. This form (I1) of interaction set was used in previous simulation studies of amphiphilic aggregation, as well as in the initial work by R. Larson which focussed on ordered mesophases which occur at high (liquid-like) amphiphilic volume fractions. The second interaction set we study (denoted I2) has HH, HT, and TT nearest-neighbor interactions given by $[+2,+1,-2]$, respectively; as for the I1 set, positive/negative interaction energies correspond to repulsive/attractive interactions. Interaction set I2 thus includes repulsive HH and HT interactions over and above the excluded volume restriction. The temperature scale is in both cases set by the energy units employed in the interaction sets.

We performed Monte Carlo (MC) simulations of the one-component amphiphile system in the grand ensemble. The move types employed include insertion and removal of chains, chain conformational renewal by reptation moves, and also translational moves of connected amphiphile “clusters”. The insertion/removal of chains was performed using the athermal configuration-bias technique to permit chain insertions without overlapping with pre-existing occupied sites. Amphiphile “clusters” are identified as sets of chains such that every included chain shares in at least one nearest-neighbor TT inter-chain contact with another (distinct) chain contained in the same cluster. We typically employed 50 % transfer (chain insertion or removal), 49.9 % reptation-type, and 0.1 % cluster moves in the course of a run; the moves resulting in displacement of a connected cluster are computationally relatively expensive, and hence attempted infrequently. Systems were equilibrated at each temperature and chemical potential over a period of $10 - 30 \times 10^6$ MC steps, followed by collection of data over a subsequent period of $30 - 50 \times 10^6$ steps. Simulation runs were performed at a series of different temperatures and chemical potential (μ) for each interaction set; histograms of the frequencies of occurrence of total amphiphile numbers and total system energy were combined and re-weighted to obtain estimates of the grand partition function, and hence the compressibility factor, as functions of the temperature and imposed chemical potential:

$$\frac{PV}{k_B T} = \ln \Xi = \ln \left(\sum_{N,E} e^{(N\mu - E)/k_B T} \right), \quad (1)$$

where Ξ is the grand canonical partition function. As has been pointed out previously [9], significant hysteresis effects exist at low enough temperatures, with the state of aggregation (micellized or dispersed) and number of micelles observed being roughly constant over an entire run.

From the combined histograms, we determined the volume fraction occupied by amphiphiles and the compressibility factor as functions of the chemical potential. The same calculation allows determination of the compressibility factor as a function of amphiphile volume fraction at a given temperature. Simulation runs were performed for each temperature at a low enough chemical potential that the ideal gas behavior was recovered explicitly for low enough amphiphile volume fractions. At sufficiently low temperatures (as discussed in greater detail subsequently), the ideal gas behavior breaks down as the amphiphile volume fraction is raised, giving way to a weaker but still demonstrably linear growth in the pressure with equilibrium amphiphile volume fraction. This weaker growth in pressure with amphiphile volume fraction is due to the incipient aggregation into micellar clusters, which leads to a net decrease in the number of independent kinetic entities in the simulation box relative to the scenario in which all the amphiphiles are dispersed and unclustered. At high enough volume fractions of amphiphile, this second linear regime for the growth of the pressure eventually breaks down. The amphiphile volume fraction at the crossover between ideal gas behavior and the weaker, but still linear, pressure growth regime is determined by the intersection of piecewise linear fits to the pressure-volume fraction curves in both regimes; this concentration is employed as an operational estimate of the temperature-dependent CMC for our model system. Examples of the dependence of the compressibility factor on amphiphile volume fraction and temperature are shown in Fig. 1.

As discussed in more detail in the following section, our model exhibits a clearly identifiable CMC-like concentration only if the temperature is below a certain critical upper bound. As the temperature rises, the slope of the pressure-volume fraction curve in the secondary linear regime becomes larger, and eventually it becomes difficult to clearly distinguish this from the ideal gas regime. The present work regards an acceptably clear demarcation of the CMC as being possible so long as the slope of the pressure in this secondary concentration regime is no larger than 0.1. As mentioned in the Introduction, it is to be noted that precise location of the CMC depends on the property whose dependence on surfactant concentration is used to characterize the aggregation process (for polydisperse aggregates). Use of a metric other than the osmotic pressure may thus lead to a slight change in the CMC location even within the present model, but its dependence on temperature and choice of interaction set is not expected to be affected.

The following section presents results for the temperature dependence of the observed CMC for the I1 and I2 interaction sets, and for the enthalpic

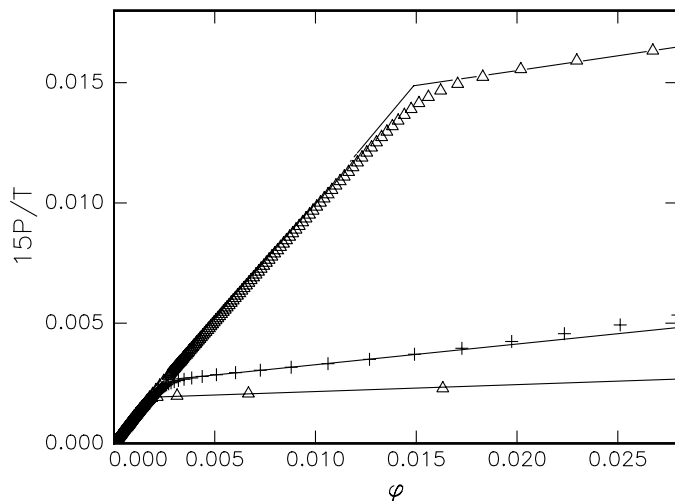


Fig. 1. The quantity $15P/k_B T$ as a function of the amphiphile volume fraction, ϕ , for H_9T_6 chains. The triangles show results for the I1 interaction set at $T = 6$ (upper) and $T = 5$ (lower); the crosses show results for the I2 interaction set at $T = 6.5$. The straight line segments at low amphiphile volume fraction correspond to ideal gas behaviour, while at higher volume fractions, the best linear fit to the secondary regime where P increases linearly with ϕ is shown.

and entropic contributions to the free energy of micellization. Results for the micellar sizes, size distributions and radii of gyration are also presented.

3 Results

3.1 Critical Micelle Concentration (CMC)

GCMC simulation results for the CMC at various temperatures for the I1 interaction set, in which the amphiphiles were placed on a $30 \times 30 \times 30$ sized simulation cell, are presented in Table 1; corresponding results for the I2 interaction set, also obtained for a $30 \times 30 \times 30$ sized cell, are shown in Table 2.

The results in Tables 1 and 2 show that: (i) for *both* interaction sets I1 and I2, the CMC concentration increases with increasing temperature, and (ii) that the absolute values of ϕ_{cmc} are significantly reduced for the I2 interaction set as compared to values obtained using the interaction set I1. The observed increase in ϕ_{cmc} with increasing temperature in our model is qualitatively consistent with the experimental trend found for non-ionic surfactants of the n-alkyl m-oxyethylene form in weakly polar solvents, e.g., formaldehyde, and for α -monoolein in nonpolar solvents like benzene or cyclohexane [15]. However, this is inconsistent and of opposite nature to what

Table 1. Amphiphile volume fractions (ϕ_{cmc}) and chemical potentials (μ_{cmc}) at the CMC for interaction set I1 as a function of temperature T; also shown is the slope s of the compressibility factor as a function of amphiphile volume fraction in the secondary linear regime with amphiphile concentrations just above the CMC.

T	ϕ_{cmc}	μ_{cmc}	s
5	0.00193	-44.2	0.028
5.5	0.00626	-42.1	0.049
5.6	0.00758	-41.7	0.063
5.7	0.00906	-41.4	0.075
5.8	0.0108	-41	0.087
5.9	0.0127	-40.7	0.104
6	0.0149	-40.4	0.123
6.5	0.0312	-38.8	0.207

Table 2. Amphiphile volume fractions ϕ_{cmc} and chemical potentials μ_{cmc} at the CMC for interaction set I2 as a function of temperature T; also shown is the slope s of the compressibility factor as a function of amphiphile volume fraction in the secondary linear regime with amphiphile concentrations just above the CMC.

T	ϕ_{cmc}	μ_{cmc}	s
5.5	0.00030	-50.8	0.035
6	0.00098	-48.2	0.057
6.5	0.0026	-45.7	0.086
6.6	0.0032	-45.2	0.093
6.7	0.0037	-44.8	0.107
6.8	0.0043	-44.3	0.123
6.9	0.0050	-43.9	0.134
7	0.0056	-43.6	0.177
7.5	0.0118	-40.9	0.256

is found experimentally for surfactant molecules of the n-alkyl m-ethoxyl family in aqueous solutions, for which the CMC is known to decrease with increasing temperature [14]. The reason for this qualitative inconsistency with the experimentally observed behavior of non-ionic surfactants of the C_nE_m family in water becomes clearer upon performing straight-line fits to the

logarithm of ϕ_{cmc} versus $1/T$, the slopes and intercepts of these fits yielding the enthalpy and entropy of micellization:

$$\ln(\phi_{cmc}) = \frac{\delta G_{mic}}{k_B T} = \frac{\delta H_{mic}}{k_B T} - \frac{\delta S_{mic}}{k_B}, \quad (2)$$

where δG_{mic} , δH_{mic} , and δS_{mic} are the standard Gibbs free energy, enthalpy, and entropy of micellization per amphiphile molecule, respectively. (The volume fraction of the pure solvent/“water” has been equated to unity in applying the result due to Molyneux et. al. [16]). The logarithm of ϕ_{cmc} is shown as a function of $1/T$ for both interaction sets I1 and I2 in Fig. (2); the fitted straight lines yield: $\delta H_{mic} \approx -60.1$, $\delta S_{mic} \approx -5.83k_B$ for the I1 interaction set, and $\delta H_{mic} \approx -75.2$, $\delta S_{mic} \approx -5.60k_B$ for interaction set I2. In both cases, both the entropy and enthalpy of micellization is found to be negative, i.e., the formation of aggregates is an energetically favorable, but entropically hindered process. Based on the operational criterion that a well-defined CMC is to be identified only under conditions such that the slope of the compressibility factor as a function of amphiphile volume fraction does not exceed 0.1 in the secondary linear regime which follows the ideal-gas like behavior, there exists an “upper critical micellization temperature” at about $T \approx 5.9 \pm 0.1$ for the I1 and $T \approx 6.7 \pm 0.1$ for the I2 interaction sets.

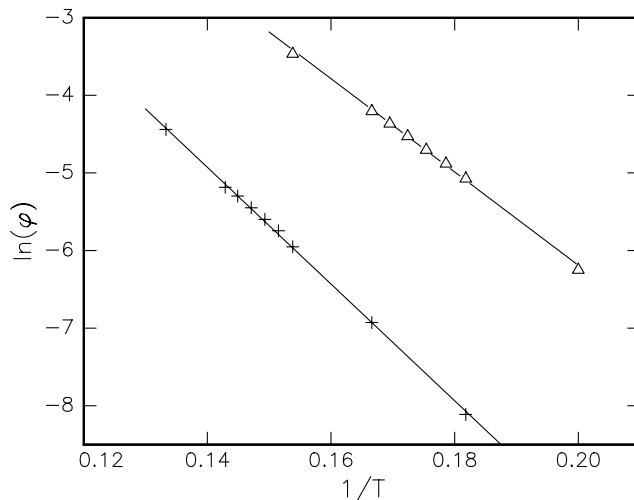


Fig. 2. $\ln(\phi_{cmc})$ is plotted as a function of $1/T$ for the I1 (triangles) and I2 (crosses) interaction sets; the lines are linear fits using the values of δH_{mic} and δS_{mic} discussed in Section III.

The absolute values of the CMC found for the model H_9T_6 molecule for both interaction sets are somewhat higher than the experimentally de-

terminated CMC for the $C_{12}E_8$ amphiphile in water. For example, at room temperature (298 K), $C_{12}E_8$ in water has a CMC of about $7.1 \times 10^{-5} \text{M}$; if we use the mapping that each unit cell on our lattice corresponds to a volume of roughly 60\AA^3 , this concentration corresponds to an amphiphile volume fraction of $\phi_{cmc} \approx 3.8 \times 10^{-5}$. Thus, at the lowest temperatures studied presently, the CMC values for our H_9T_6 model exceed the experimental room temperature values for $C_{12}E_8$ by factors of about 8 and 50 for the I2 and I1 interaction sets, respectively. Inclusion of repulsive head-head and head-tail interactions significantly lowers the absolute value of the model CMC in the range of temperature we have been able to study, and brings it closer to the experimental range of values at room temperature, but it is still too large by a significant factor.

Our present results for the enthalpic contribution to the free energy of micellization for the I1 case may be compared with the findings of earlier work on amphiphiles of the H_3T_3 and H_4T_4 architectures, which had employed an I1-like interaction set specified by [0,0,-2] for the HH, HT, and TT interactions, respectively. Taking together the earlier and present results for δH_{mic} for H_3T_3 , H_4T_4 , and H_9T_6 surfactant molecules, the quantity $\delta H_{mic}/\epsilon_{TT}$ varies in the ratio of approximately 3:4:5.7 for this set of architectures. Thus, for interaction sets of the I1 type, the enthalpy of micellization is approximately proportional to the number of interacting tail groups per surfactant, and always favors aggregation. The slightly more positive value for $\delta H_{mic}/|\epsilon_{TT}|$ for the I2 with respect to the I1 interaction sets for H_9T_6 (-37.6 versus -45.2) reflects the head-head and head-tail repulsive interactions which are augmented when the head group segments of aggregated chains are forced to inhabit the corona region surrounding the micellar core. Examination of earlier and present results (for the I1 case) for the entropy of micellization δS_{mic} per amphiphile reveal that, for the H_3T_3 , H_4T_4 , and H_9T_6 set of amphiphiles, the findings are consistent with a linear dependence of $\delta S_{mic}/k_B$ on the number of tail groups N_T *alone*:

$$\frac{\delta S_{mic}}{k_B} = -1.18 - 0.77N_T. \quad (3)$$

Note that this quantity is (at least for the H_9T_6 molecule of the present study) *not* dramatically altered on going from the I1 to the I2 interaction set, suggesting that the major entropic contribution in the micellization process stems from the re-organization of tail group segments on going from the dispersed to micellar core regions. These remarks should be regarded as merely suggestive, as they are based on results for only four combinations of amphiphile architecture and interaction set. In all cases, the entropic contribution favors amphiphilic dispersion rather than aggregation.

For the experimentally relevant n-alkyl m-ethoxyl surfactants, precisely the *opposite* situation is known to be true [14]; thus, δH_{mic} and δS_{mic} are *both* positive, indicating that the formation of aggregates is an entropically rather than energetically-driven process. The underlying source for this phenomenon

is the “hydrophobic effect”, first studied in detail by Frank and Evans [17] in the context of the water solubility of simple, non-ionic molecules. Our present model does not do justice to the structure of water as a hydrogen-bonded, networked fluid; in particular, the potential for formation of “icebergs” in the water domains surrounding dispersed amphiphile molecules, leading to a locally more ordered and hence lower entropy structure, is not captured by a simple model in which water molecules are represented as sites interacting via purely isotropic nearest-neighbor interactions. The fact that we find δH_{mic} to be negative for our model for both interaction sets is consistent with the situation that in either case, the formation of aggregates must be accomplished based on purely energetic considerations. In recent years, a number of models for water have been proposed which incorporate these aspects relevant to a faithful description of the aggregation phenomenon in aqueous environment [18]. The use of such models for the solvent/”water” together with our present treatment of the amphiphilic molecules may be expected to yield results in closer qualitative accord with experiment, and shall be pursued in future work on this subject.

3.2 Aggregate Size

Results for the oligomer and micellar volume fractions and micellar aggregation numbers, $\langle M \rangle$ are shown in Tables 3 and 4 for the I1 and I2 interaction sets, respectively. In each case, the cluster size distribution (frequency of occurrence of clusters of a given size) was obtained from a GCMC run equilibrated at the relevant values of T and μ , and the peak found at higher values of M was fitted to a Gaussian distribution. The standard deviation of the Gaussian fitted curves, W , are also shown on Tables 3 and 4. Also shown in Tables 3 and 4 are the mean values of the three principal radii of gyration as calculated from snapshots of the bead coordinates, averaged over all clusters containing more than 10 amphiphile molecules. The location of the center of mass of the micelle is calculated by assigning equal weights to head and tail group segments. The error estimates in the tables represent standard deviations of results from four independent runs.

The results in Tables 3 and 4 show that, as estimated from the radii of gyration, the micellar dimensions are roughly similar for both interaction sets studied; however, the mean aggregation number is significantly lower for the I2 interaction set. For both interaction sets, a systematic decrease in the micelle size is found with increasing temperature. This is consistent with our observation that, above an “upper critical micellization temperature,” we do not find formation of stable micellar aggregates for either the I1 or I2 interaction sets, as the aggregation process is energetically driven for the present model.

Table 3. Mean micellar aggregation numbers $\langle M \rangle$, averaged values of the principal radii of gyration, and dispersed amphiphile (oligomeric clusters) and micellar volume fractions ϕ_{olig} and ϕ_{mic} for interaction set I1. Numbers in parentheses indicate error estimates (one standard deviation) in the last digit, where available.

T	μ	ϕ_{olig}	ϕ_{mic}	$\langle M \rangle$	W	$R_g^{(1)}$	$R_g^{(2)}$	$R_g^{(3)}$
5.5	-41.5	0.0058(0)	0.031(1)	56(2)	9.3	5.17(8)	4.98(7)	4.69(7)
5.5	-41.1	0.0061(2)	0.036(3)	66(5)	9.7	5.4(1)	5.1(1)	4.9(1)
5.5	-41	0.0064(0)	0.037(1)	67(2)	10.2	5.36(6)	5.17(5)	4.90(6)
5.5	-40.9	0.0053(2)	0.073(3)	66(2)	10.0	5.34(8)	5.1(1)	4.89(9)
5.5	-40.6	0.0040(2)	0.114(6)	70(4)	10.4	5.45(7)	5.25(7)	5.00(7)
6	-39.6	0.019(1)	0.009(6)	46(4)	9.2	4.8(2)	4.7(2)	4.3(3)
6	-39	0.015(2)	0.05(2)	51(2)	9.7	5.13(6)	4.91(8)	4.60(7)
6.5	-37	0.034(2)	0.042(6)	37(1)	11.0	4.9(1)	4.65(9)	4.23(4)

Table 4. Mean micellar aggregation numbers $\langle M \rangle$, average values of the principal radii of gyration, and dispersed amphiphile (oligomeric clusters) and micellar volume fractions ϕ_{olig} and ϕ_{mic} for interaction set I2. Numbers in parentheses indicate error estimates (one standard deviation) in the last digit where available.

T	μ	ϕ_{olig}	ϕ_{mic}	$\langle M \rangle$	W	$R_g^{(1)}$	$R_g^{(2)}$	$R_g^{(3)}$
5	-51.4	0.000027(1)	0.067(2)	42(2)	4.1	5.48(6)	5.31(8)	5.05(8)
5.5	-49.4	0.00026(1)	0.0184(7)	33(2)	4.7	5.23(4)	5.05(4)	4.80(4)
5.5	-49.3	0.00025(1)	0.028(3)	49(6)	5.9	5.8(2)	5.6(2)	5.4(2)
5.5	-49.2	0.00022(1)	0.030(2)	54(4)	3.5	5.91(8)	5.8(1)	5.55(8)
5.5	-48.9	0.00019(1)	0.043(3)	38(2)	3.8	5.42(9)	5.3(1)	5.03(8)
5.5	-46.5	0.00012(2)	0.082(6)	50(2)	4.3	5.7(1)	5.5(1)	5.3(1)
6.5	-43.3	0.0019(1)	0.038(3)	35(3)	5.4	5.3(1)	5.1(1)	4.9(1)
6.5	-43	0.0013(2)	0.056(2)	35(1)	5.4	5.31(4)	5.11(4)	4.86(3)
6.5	-42	0.0013(1)	0.063(2)	38(1)	5.0	5.45(5)	5.26(4)	5.01(4)
7	-40.5	0.0046(5)	0.036(5)	31(2)	5.0	5.2(1)	4.9(1)	4.7(1)
7	-38.5	0.0028(8)	0.069(8)	36(1)	6.0	5.35(7)	5.14(6)	4.90(7)
7.5	-38	0.0083(7)	0.040(4)	29(1)	5.9	5.08(3)	4.84(4)	4.53(5)
7.5	-37.5	0.008(2)	0.047(9)	29(1)	5.2	5.11(7)	4.88(7)	4.59(8)
7.5	-35.5	0.0051(9)	0.073(4)	34(1)	5.4	5.28(6)	5.05(7)	4.76(9)

4 Discussion

The thermodynamics of amphiphile aggregation into approximately spherical micelles has been investigated for a linear, asymmetric, model surfactant molecule on a lattice for two different sets of microscopic interaction parameters. Results for the CMC, and the enthalpy and entropy of micellization, have been compared to previous simulation results for shorter-chain, symmetric surfactant molecules. Issues relating to the micellar size (in terms of both mean aggregation number and radii of gyration) and structure (quantified by density profiles and orientational order parameters for the molecular bond vectors), together with a comparison to predictions of single chain mean-field theory, shall be addressed in a future work.

The primary result of the present work has been to show that the enthalpy and entropy of micellization are approximately linear in the number of interacting groups per molecule, for both symmetric and asymmetric architectures. In addition, we find that alteration of the microscopic pairwise interaction strengths can significantly impact the CMC concentration; this may be of great relevance to future studies designed to more closely approximate the situation in real aqueous surfactant assemblies. However, the qualitative dependence of CMC on temperature was not altered for the two interaction sets considered here, and remains at variance with the experimental trend known for the alkyl-ethoxyl family of amphiphiles in water. As discussed previously, we believe this inconsistency is a consequence of the present treatment of water as a structureless, single-site vacancy, which neglects the complex orientation and local density-dependence of the hydrogen bonding network characteristic of water at room temperatures. Consideration of more realistic lattice models for water, which incorporate aspects of the hydrophobic effect, is currently under way, and is expected to improve agreement with at least the qualitative features observed experimentally when used in conjunction with the present models for the surfactant-only system.

References

1. Tanford, C. (1980) *The hydrophobic Effect*. Wiley, New York.
2. Schick, M. J. (1987) *Nonionic Surfactants; Physical Chemistry*. Marcel Dekker, New York.
3. Rosen, M.J. (1989) *Surfactants and Interfacial Phenomena*. 2nd Ed., John Wiley, New York.
4. Israelachvili, J. (1992) *Intermolecular and Surface Forces*. 2nd Ed. Academic Press, London.
5. Von Gottberg, F. K., Smith, K. A., Hatton, T. A., (1997) Stochastic Dynamics Simulation of Surfactant Self-assembly. *J. Chem. Phys.* **106**, 9850-7.
6. Mackie, A. D., Panagiotopoulos, A. Z., Szeleifer, I. (1997) Aggregation Behavior of a Lattice Model for Amphiphiles. *Langmuir* **13**, 5022-31.

7. Xing, L., Mattice, W. L. (1997) Strong Solubilization of Small Molecules by Triblock-Copolymer Micelles in Selective Solvent. *Macromolecules* **30**, 1711-1717.
8. Viduna, D., Milchev, A., Binder, K. (1998) Monte Carlo Simulation of Micelle Formation in Block Copolymer Solutions. *Macromolecular Theory Simul.* **7**, 649-58.
9. Floriano, M. A., Caponetti, E., Panagiotopoulos, A. Z. (1999) Micellization in Model Surfactant Systems. *Langmuir*, in press.
10. Almdal, K., Bates, F. S., Mortenson, K. (1992) Order, disorder, and Fluctuation Effects in an Asymmetric Poly (ethylene-propylene)-poly (ethylene) Diblock Copolymer. *J. Chem. Phys.* **96**, 9122-32.
11. Ferrenberg, A. M., Swendsen, R. H. (1988) New Monte Carlo Technique for Studying Phase Transitions. *Phys. Rev. Lett.* **61**, 2635-8.
12. Leibler, L. (1980) Theory of Microphase Separation in Block Copolymers. *Macromolecules* **13**, 1602-17.
13. Larson, R. G., Scriven, L. E., Davis, H. T. (1985) Monte Carlo simulation of amphiphile-oil-water systems. *J. Chem. Phys.* **83**, 2411-20.
14. Meguro, K., Takasawa, Y., Kawahashi, N., Tabata, Y., Ueno, M. (1981) Micellar Properties of a Series of Octaethyleneglycol-n-alkyl Ethers with Homogeneous Ethylene Oxide Chains and their Temperature Dependence. *J. Coll. Interface Sci.* **83**, 50-56.
15. Kon-no, K., Jin-no, T., Kitahara, A. (1974) Solubility, Critical Aggregating or Micellar Concentration, and Aggregate Formation of Nonionic Surfactants in Nonaqueous Solutions. *J. Coll. Interface Sci.* **49**, 383-89.
16. Molyneux, P., Rhodes, C. T., Swarbrick, J. (1965) Thermodynamics of Micellization of N-Alkyl Betaines. *Trans. Faraday Soc.* **61**, 1043-52.
17. Frank, H. S., Evans, M. W. (1945) Free Volume and Entropy in Condensed Systems - III. *J. Chem. Phys.* **13**, 507-32.
18. Roberts, C. J., Panagiotopoulos, A. Z., Debenedetti, P. G. (1996) Liquid-Liquid Immiscibility in Pure Fluids: Polyamorphism in Simulations of a Network-Forming Fluid. *Phys. Rev. Lett.* **77**, 4386-89; Roberts, C. J., Debenedetti, P. G. (1996) Polyamorphism and density anomalies in network-forming fluids: Zeroth- and first-order approximations. *J. Chem. Phys.* **105**, 658-72, and references therein.